OPEN

Green Synthesis of ZnO Nanoparticles using Pomegranate Peel Extract and Evaluation of their Antimicrobial and Antibiofilm Activity

Singh Mehak[1]*, Taiwade Latasha[2] & Shanware Arti[2]

The increasing prevalence of antimicrobial resistance and biofilm-associated infections has created an urgent need for sustainable antimicrobial agents with enhanced efficacy and reduced environmental impact. In the present study, zinc oxide nanoparticles (ZnO NPs) were synthesized through an eco-friendly green synthesis approach using aqueous peel extract of *Punica granatum* L. as a natural reducing and capping agent. Zinc acetate dihydrate served as the precursor, and the synthesized nanoparticles were characterized using UV–Visible spectroscopy, Fourier Transform Infrared (FTIR) spectroscopy and scanning electron microscopy (SEM). UV–Visible analysis showed characteristic absorption peaks consistent with nanoparticle formation, while FTIR spectra revealed the presence of phytochemical functional groups along with Zn–O stretching vibrations, consistent with the association of bioactive compounds from the peel extract with the nanoparticles. SEM showed irregular particles and aggregates with lengths of 164–1,083 nm (mean 559 ± 217 nm; n = 60), and primary particle size could not be resolved at the magnification used. The antimicrobial activity of the synthesized ZnO NPs was evaluated against *Staphylococcus aureus* and *Klebsiella pneumoniae* using the agar well diffusion assay, whereas antibiofilm activity was assessed by the crystal violet microtiter plate assay. The nanoparticles exhibited concentration-dependent zones of inhibition and reduced crystal-violet-stained biofilm biomass against both bacterial strains. The highest antibacterial activity was observed at 20 mg/mL, producing inhibition zones (total diameter including the 6 mm well) of 25 mm against *K. pneumoniae* and 13 mm against *S.aureus*. Similarly, maximum reduction in crystal-violet-stained biomass reached 87.14% for K. pneumoniae and 75.39% for S. aureus at a final concentration of 2.0 mg/mL (20 mg/mL. stock). Overall, the findings demonstrate that P. granatum peel-mediated ZnO nanoparticles showed preliminary antimicrobial and biofilm-reducing potential, highlighting the value of agricultural waste in the sustainable production of biocompatible nanomaterials for prospective biomedical and antimicrobial applications. Further structural characterization and mechanistic investigations are recommended to strengthen their potential for clinical and industrial use. This work is preliminary: XRD, MIC and growth or viability controls were not performed, SEM was limited to a single micrograph, and one strain per species was tested.

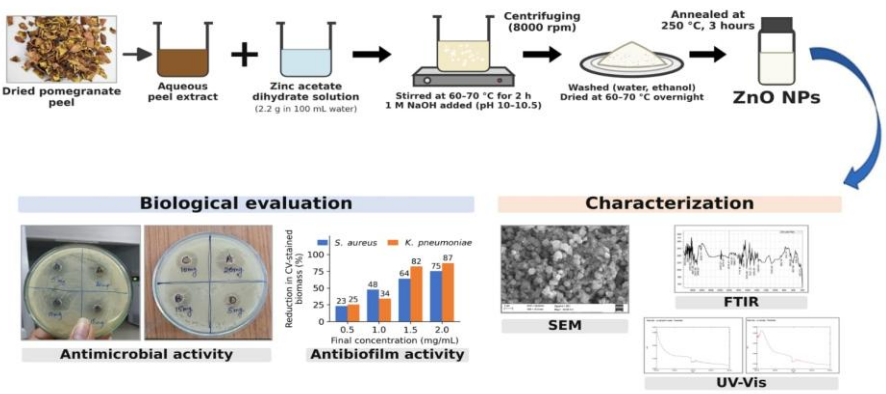


Figure 1. Schematic illustration of ZnO NPs preparation using pomegranate peel extract

1. Amity Institute of Biotechnology, Amity University Mumbai, Mumbai-Pune Expressway, Bhatan, Post-Somathne, Panvel, Maharastra – 410206, India
2. Rajiv Gandhi Biotechnology Centre, Laxminarayan Innovation Technological University (LITU), Amravati Road, Ram Nagar, Nagpur, Maharashtra - 440033, India[1]. *mehak.s.0506@gmail.com; Phone: +91 885042813

Antibiotic resistance poses a critical challenge to global healthcare infrastructure, driven largely by the misuse of conventional antimicrobial drugs, creating an urgent need for the development of alternative antimicrobial agents with novel mechanisms that are non-toxic to human cells, inexpensive, and environmentally acceptable as bactericidal agents.

This clinical challenge is compounded by the formation of biofilms, which represent the prevalent mode of microbial growth, facilitating microorganisms to survive as highly organized communities rather than individual free-floating cells [1]. A biofilm is an organized microbial aggregate enclosed within a self-produced extracellular polymeric substance (EPS) matrix. They are composed of polysaccharides, nucleic acids, lipids, proteins, water, and ions, providing structural support and protection to the microbial community. Once fully established, mature biofilms become highly resilient to antimicrobial therapies and host immune systems, as the EPS matrix restricts the diffusion of antibiotics and immune cells while quorum sensing facilitates the exchange of nutrients and resistance genes [2]. Consequently, microorganisms within a biofilm can survive antimicrobial exposures far greater than those required to eliminate free-floating planktonic cells, resulting in chronic infections that are difficult to treat with standard therapies.

Nanotechnology introduces a viable alternative to conventional therapies by utilizing materials with dimensions ranging from 1 to 100 nanometers [3,4]. At this scale, nanomaterials exhibit enhanced mechanical, thermal, magnetic, electronic, optical, and catalytic properties compared to bulk materials due to the surface and quantum effects. Among inorganic nanoparticles, metal oxide NPs such as ZnO, TiO_2, CuO, MgO, Fe_2O_3, and Al_2O_3 form an important class, exhibiting high chemical stability, good biocompatibility, photocatalytic activity, and antimicrobial properties [5,6]. Among these, ZnO NPs are particularly promising.

In this work, we utilized *Punica granatum L.* (pomegranate) peel to prepare the nanoparticles in a more sustainable and biocompatible way. Peel makes up around 30-40% of the fruit's weight and is usually just thrown away during processing. However, the peel is highly enriched in polyphenolic acids, ellagic acid, punicalins, punicalagin, and flavonoids such as catechins, quercetin, kaempferol, anthocyanins, and rutin. These phytochemicals act as natural reducing, capping, and stabilizing agents during the biosynthesis of ZnO nanoparticles. Specifically, their hydroxyl (-OH) and carbonyl (C=O) functional groups interact with the Zn^{2+} ions derived from the metal precursor to drive nanoparticles nucleation under optimal conditions [7]. This contributes to better control over the size and morphology of the nanoparticles. Consequently, these particles demonstrate high stability, biodegradability, versatile surface chemistry, and intrinsic biocompatibility. The abundant phytochemical profile positions *P. granatum* peel an ideal candidate for green synthesis of ZnO NPs [8,9,10,11]. ZnO NPs exhibit unique physicochemical properties, including a high surface-area-to-volume ratio, strong chemical stability, photocatalytic activity, UV absorption capability, and broad-spectrum antimicrobial activity, making them promising materials for biomedical, environmental, and antimicrobial applications [12,13].

In contrast, conventional NP synthesis relies on hazardous reducing agents, solvents, and synthetic stabilizers, that are often toxic, expensive, and environmentally harmful, and typically requires high-energy procedures that increase the overall environmental footprint [14]. The phytochemical-mediated approach overcomes these limitations by utilizing renewable plant-derived biomolecules, eliminating the need for additional chemical reagents, and offers a simpler, more cost-effective, and lower-impact route to ZnO NPs with good physicochemical properties and biocompatibility [15,16].

Results and Discussion

Green Synthesis of ZnO Nanoparticles

The green synthesis of zinc oxide nanoparticles was carried out using the aqueous peel extract of *Punica granatum* and zinc acetate dihydrate as the precursor. During the synthesis, the reaction mixture gradually developed a whitish precipitate following the addition of sodium hydroxide and continuous stirring, indicating the formation of ZnO nanoparticles. The precipitate was separated by centrifugation, washed with distilled water and ethanol, oven dried, and annealed at 250 °C for 3 hours to obtain a fine powdered product, yielding approximately 1.37 g of ZnO nanoparticles.

UV–Visible Spectrophotometric Analysis

The synthesized ZnO nanoparticles were characterized using UV–Visible spectrophotometry over a wavelength range of 200–400 nm (Figures 2 and 3). The distilled water dispersion exhibited absorption peaks at 202.8 nm and 261.4 nm, with absorbance values of 1.577 and 0.549, respectively, while the methanolic dispersion showed a prominent peak at 212.6 nm (absorbance 3.073) along with additional peaks at 248.8, 296.4, 331.2, 353.4, and 367.4 nm. Since ZnO nanoparticles synthesized via green, plant-mediated routes have been

reported to show a red-shift and narrowing of the optical band gap compared to conventionally synthesized ZnO NPs, attributed to surface functionalization by phytochemicals from the plant extract [22], some variation from the characteristic ZnO absorption range is expected in phytochemically capped nanoparticles such as those synthesized in this study. The peaks recorded at 331.2 nm and 367.4 nm in the methanolic dispersion, closer to the commonly reported ZnO absorption window, are considered more representative of the synthesized ZnO nanoparticles, while the dominant peaks observed at comparatively lower wavelengths in both dispersions are likely attributable to residual phenolic and flavonoid compounds from the *P. granatum* peel extract that remained adsorbed onto the nanoparticle surface as capping agents [23].

Fourier Transform Infrared (FTIR) Spectroscopic Analysis

The FTIR spectrum of the synthesized ZnO nanoparticles (Figure 4) exhibited characteristic absorption bands at approximately 3230.77, 1687.71, 1541.12, 1456.26, 1363.67, 1070.49, 862.18, 754.17,669.30, 607.58, 538.14, and 453.27 cm^{-1}. The broad band at 3230.77 cm^{-1} corresponds to O–H stretching of phenolic hydroxyl groups and adsorbed water, while bands at 1687.71 and 1541.12 cm^{-1} are attributed to C=O stretching and N–H bending, respectively, and those at 1456.26 and 1363.67 cm^{-1} correspond to C–H bending and C–N stretching. These bands, along with their positions, are consistent with the functional group profile reported for pomegranate-peel-mediated ZnO nanoparticles, where similarly broad O–H/N–H bands and C=O/N–H stretching regions have been attributed to residual phytochemicals from the peel extract acting as capping agents [8]. The band at 1070.49 cm^{-1} is assigned to C–O stretching of alcohols and phenolic compounds, while the prominent bands at 538.14 and 453.27 cm^{-1} are characteristic of Zn–O stretching vibrations, consistent with the formation of zinc oxide nanoparticles. Together, the spectrum revealed functional groups associated with phytochemicals from the pomegranate peel extract along with characteristic Zn–O vibrations, suggesting their possible role as reducing and capping agents during synthesis (Table 1).

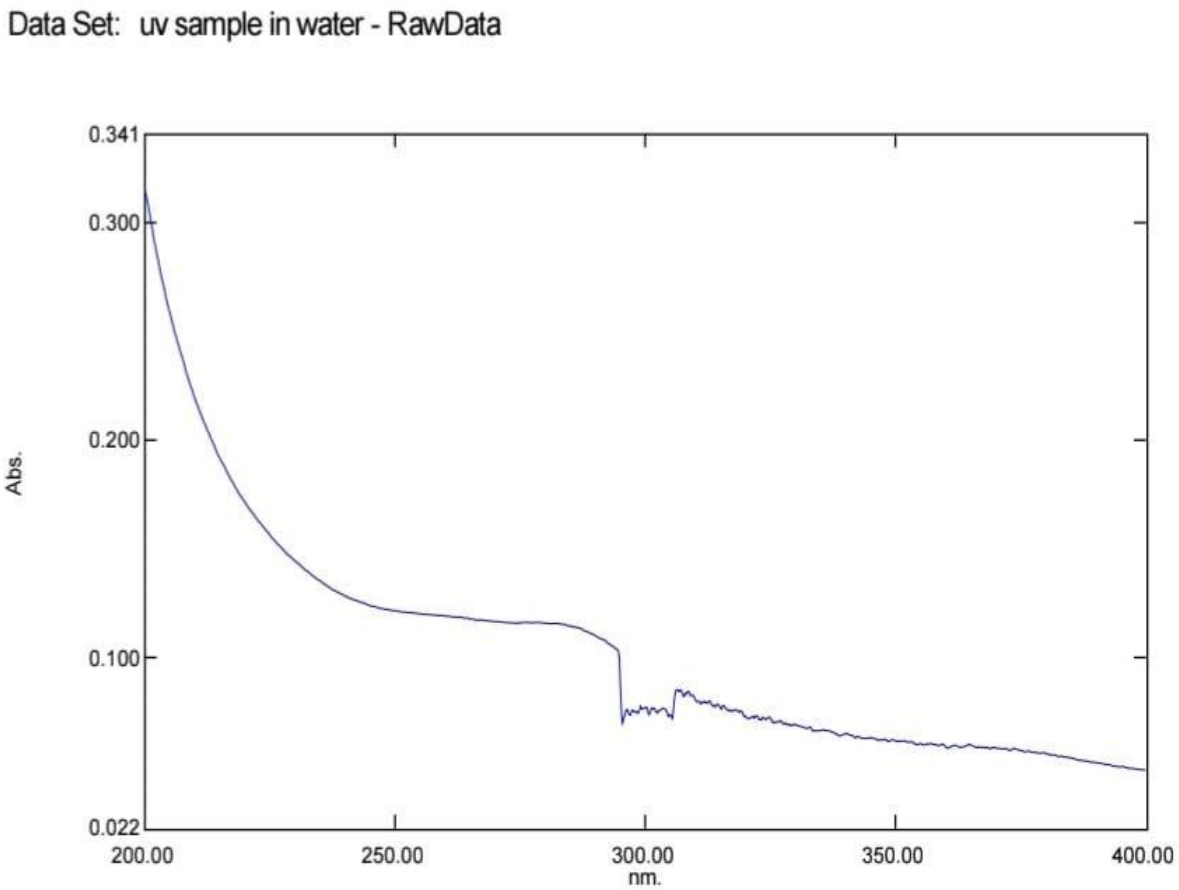


Figure 2. UV–Visible absorption spectrum of green synthesized ZnO nanoparticles dispersed in distilled water

.

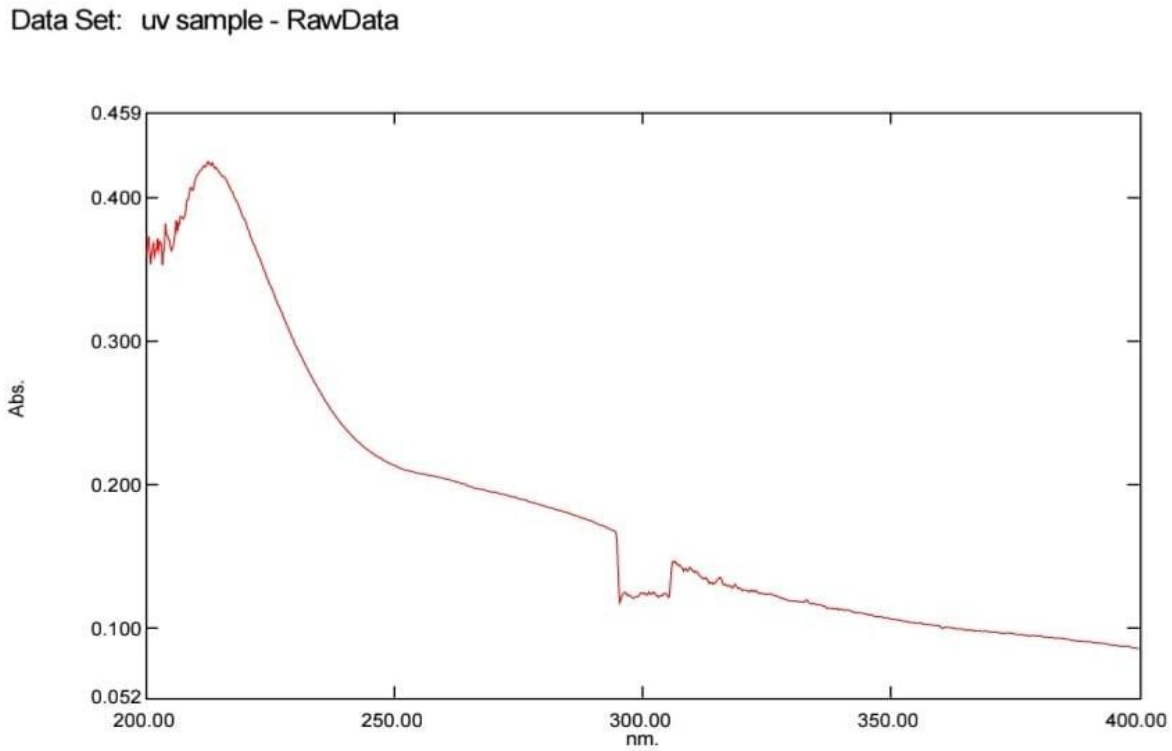


Figure 3. UV–Visible absorption spectrum of green synthesized ZnO nanoparticles dispersed in methanol.

Table 1. FTIR Spectral Data of Green-Synthesized ZnO Nanoparticles

Wavenumber (cm^{-1})	Functional Group Assignment
3230.77	O–H stretching (phenolic hydroxyl groups and adsorbed water)
1687.71	C=O stretching
1541.12	N–H bending
1456.26	C–H bending
1363.67	C–N stretching
1070.49	C–O stretching (alcohols and phenolic compounds)
538.14	Zn–O stretching vibration
453.27	Zn–O stretching vibration

Scanning Electron Microscopy (SEM) Analysis

SEM analysis (Figure 5a) showed irregular, rough-surfaced particles forming dense aggregates. Particle length, measured manually for n = 60 particles from a single micrograph (Figure 5b), ranged from 164 to 1,083 nm (mean 559 ± 217 nm; median 520 nm), and no particle below 100 nm was observed. Primary particles within the aggregates could not be resolved at ×20,000, so the size of the primary particles cannot be determined from this image. Taken together with the UV–Visible absorption features (331.2 and 367.4 nm in methanol) and the FTIR Zn–O bands (538.14 and 453.27 cm^{-1}), the SEM observations are consistent with the formation of ZnO; however, as XRD and TEM were not performed, phase identity, purity and primary particle size could not be confirmed.

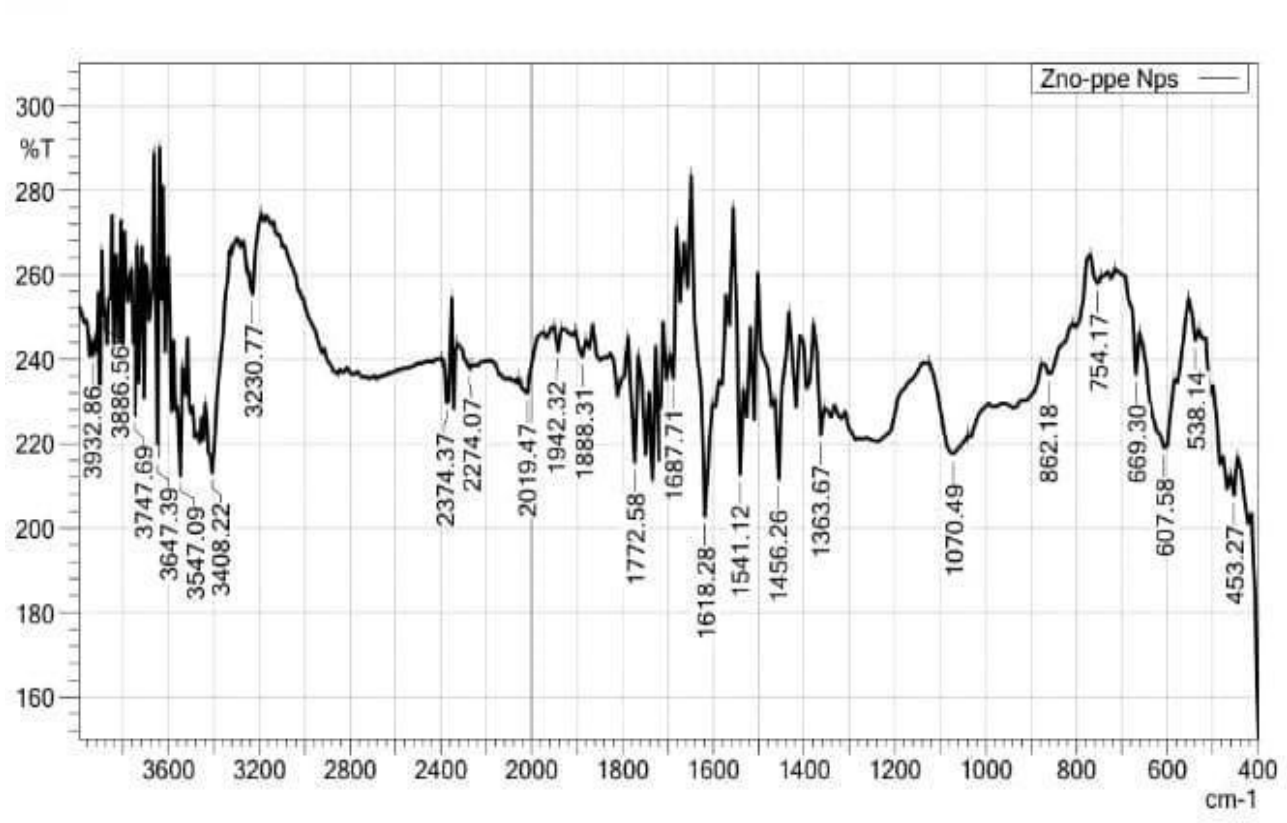


Figure 4. FTIR spectrum of green synthesized ZnO nanoparticles.

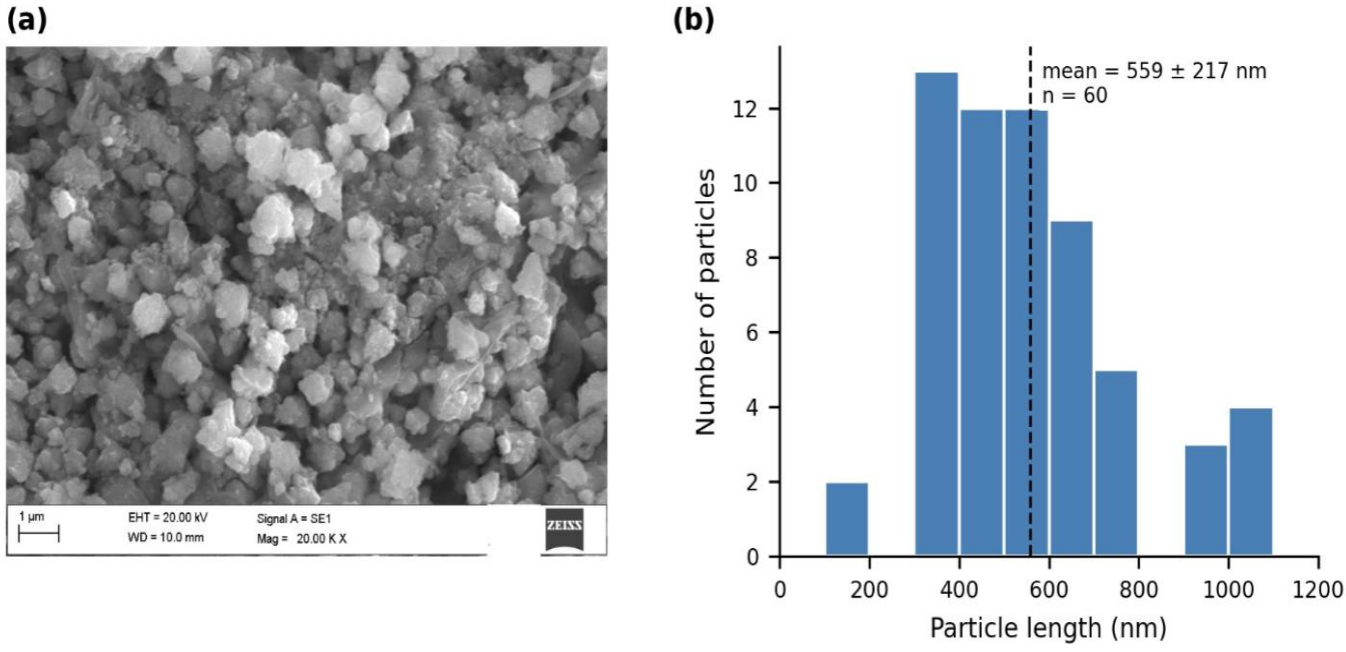


Figure 5. (a) SEM micrograph of the synthesized ZnO nanoparticles (secondary electron detector, 20 kV, ×20,000; scale bar, 1 µm). (b) Distribution of particle length measured manually in ImageJ (n = 60; mean 559 ± 217 nm)

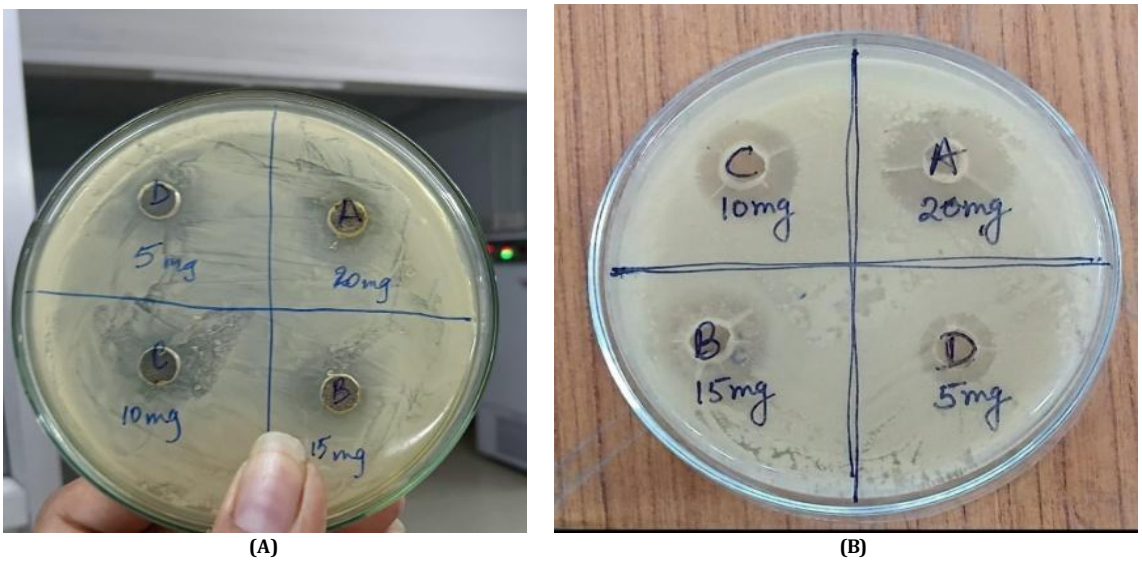
Antimicrobial Activity by Agar Well Diffusion Assay

The synthesized ZnO nanoparticles exhibited antimicrobial activity against both *Staphylococcus aureus* and *Klebsiella pneumoniae*, as evidenced by clear zones of inhibition around the wells, with the diameter of inhibition increasing with increasing nanoparticle concentration (Table 2, Figure 6).

Reported diameters include the 6 mm well. Against *K. pneumoniae*, the highest activity was observed at 20 mg/mL (25 mm), followed by 15 mg/mL (21 mm), 10 mg/mL (17 mm), and 5 mg/mL (13 mm). Against *S. aureus*, the highest activity was similarly observed at 20 mg/mL (13 mm), followed by 15 mg/mL (10 mm), 10 mg/mL (8 mm), and 5 mg/mL (7 mm). In both strains tested, the nanoparticles showed comparatively larger zones of inhibition against *K. pneumoniae* than *S. aureus*. This is a notable observation, as ZnO nanoparticles are more commonly reported to show greater antibacterial activity against Gram-positive bacteria, owing to the highly charged, anionic peptidoglycan and teichoic acid layer of their cell wall favouring electrostatic attraction to ZnO nanoparticles, whereas the thinner peptidoglycan layer and additional lipopolysaccharide-containing outer membrane of Gram-negative bacteria typically confer greater resistance [24]. The comparatively higher susceptibility of *K. pneumoniae* observed in this study may instead be attributed to strain-specific differences in outer membrane permeability or the specific concentration range tested, warranting further investigation. As only one strain per species was tested, these observations should not be generalized to Gram-positive and Gram-negative bacteria. Excluding the 6 mm well, clearing beyond the well edge was 7–19 mm for *K. pneumoniae* and 1–7 mm for *S. aureus*. Ciprofloxacin is shown for reference only; differences in format (disc versus well) and dose preclude a direct comparison. Because zone size reflects both diffusion through agar and antibacterial activity, these results indicate relative susceptibility under the assay conditions rather than potency, and the minimum inhibitory concentration (MIC) was not determined. Further optimization of the synthesis process is warranted.

Table 2. Antimicrobial activity of green synthesized ZnO nanoparticles against *Klebsiella pneumoniae* and *Staphylococcus aureus* by agar well diffusion assay

Test Sample	Concentration	Zone of Inhibition (mm) - *K. pneumoniae*	Zone of Inhibition (mm) - *S. aureus*
Ciprofloxacin	5 µg	32	31
ZnO Nanoparticles	20 mg/mL	25	13
ZnO Nanoparticles	15 mg/mL	21	10
ZnO Nanoparticles	10 mg/mL	17	8
ZnO Nanoparticles	5 mg/mL	13	7



(A) **(B)**

Figure 6. Agar well diffusion assay demonstrating the antimicrobial activity of green synthesized ZnO nanoparticles against Staphylococcus aureus (A) and Klebsiella pneumoniae (B).

Evaluation of Antibiofilm Activity by Crystal Violet Assay

The antibiofilm activity of the synthesized ZnO nanoparticles was determined against *Staphylococcus aureus* and *Klebsiella pneumoniae* using the crystal violet microtiter plate assay. Biofilm formation was quantified by measuring the absorbance of the solubilized crystal violet stain at 570 nm. For *Staphylococcus aureus*, the mean absorbance values recorded at 0.5 mg/mL, 1.0 mg/mL, 1.5 mg/mL, and 2.0 mg/mL were 0.99 ± 0.03, 0.67 ± 0.03, 0.46 ± 0.02, and 0.32 ± 0.05, respectively, while the untreated control exhibited a mean absorbance of 1.29 ± 0.02. A similar trend was observed for *Klebsiella pneumoniae*. The mean absorbance values obtained at 0.5 mg/mL, 1.0 mg/mL, 1.5 mg/mL, and 2.0 mg/mL were 0.95 ± 0.02, 0.84 ± 0.02, 0.23 ± 0.02, and 0.16 ± 0.02, respectively. The untreated control showed a mean absorbance of 1.27 ± 0.03. In both bacterial strains tested, the biofilm-associated absorbance decreased progressively with increasing nanoparticle concentration, indicating a concentration-dependent reduction in crystal-violet-stained biomass. Unlike the agar well results, biomass reduction was not consistently greater for *K. pneumoniae*. At 0.5 and 1.0 mg/mL it was similar or lower (25.46% and 34.12% versus 23.06% and 47.67% for *S. aureus*), whereas at 1.5 and 2.0 mg/mL *K. pneumoniae* showed the greater reduction (82.15% and 87.14% versus 63.99% and 75.39%). The greater reduction for *K. pneumoniae* is therefore supported only at the two highest final concentrations tested, may reflect strain-specific factors [1], and was not tested statistically. The absorbance values obtained for all experimental groups are presented in Table 3 and Table 4. Concentrations refer to the final well concentrations after tenfold dilution of the 5–20 mg/mL stock suspensions. Because the nanoparticles were present during biofilm formation and no planktonic growth or viability measurements were made, this reduction cannot be attributed specifically to antibiofilm action rather than growth inhibition, and eradication of preformed biofilms was not assessed.

Table 3. Antibiofilm activity of green synthesized ZnO nanoparticles against *Staphylococcus aureus*.

ZnO Nanoparticle Concentration (mg/mL, final)	Control OD at 570 nm (mean ± SD)	Treated OD at 570 nm (mean ± SD)	Reduction in CV-stained biomass (%)
0.5	1.287 ± 0.021	0.990 ± 0.027	23.06
1.0	1.287 ± 0.021	0.673 ± 0.025	47.67
1.5	1.287 ± 0.021	0.463 ± 0.015	63.99
2.0	1.287 ± 0.021	0.317 ± 0.045	75.39

Table 4. Antibiofilm activity of green synthesized ZnO nanoparticles against *Klebsiella pneumoniae*.

ZnO Nanoparticle Concentration (mg/mL, final)	Control OD at 570 nm (mean ± SD)	Treated OD at 570 nm (mean ± SD)	Reduction in CV-stained biomass (%)
0.5	1.270 ± 0.026	0.947 ± 0.021	25.46
1.0	1.270 ± 0.026	0.837 ± 0.015	34.12
1.5	1.270 ± 0.026	0.227 ± 0.021	82.15
2.0	1.270 ± 0.026	0.163 ± 0.015	87.14

Materials and Methods

Materials

Zinc acetate dihydrate [$Zn(CH_3COO)_2 \cdot 2H_2O$] served as the zinc precursor, and sodium hydroxide (NaOH) and used as received without further purification. All chemical reagents and solvents

utilized throughout this work were of analytical grade. Fresh *Punica granatum L.* fruits were procured from a local market in Nagpur to obtain the requisite peel precursor. Distilled water was used uniformly across all experimental stages.

Preparation of Aqueous Extract

The collected *P. granatum peels* were washed with tap water and distilled water to eliminate surface contaminants and dust. The cleaned peels were sliced and air-dried under shade at room temperature for 3 days until completely dry. Next, the dried peels were ground into a fine powder using a sterile mechanical grinder and stored in an airtight container until use. To prepare the extract, 10 g of the peel powder was added to 100 mL of distilled water and heated at 80 °C for 20 minutes. [17]. After the extract was cooled to room temperature, the solution was filtered through Whatman No. 1 filter paper, and then centrifuged at 8000 rpm for 15 minutes to remove solid residues. The clear supernatant was collected and stored at 4 °C until further use.

Biosynthesis of ZnO Nanoparticles

For green synthesis, we adapted and modified the protocols described by Fouda et al. [8] and Shaban et al. [9]. Briefly, 2.2 g of zinc acetate dihydrate [$Zn(CH_3COO)_2 \cdot 2H_2O$] was dissolved in 100 mL distilled water and heated to 60–70 °C, after which 20 mL of the peel extract was added dropwise. 1 M NaOH was then added gradually until the pH reached 10–10.5, and the mixture was stirred at 60–70 °C for 2 hours, during which a whitish precipitate formed, along with a gradual colour change from pale yellow to white. This colour change served as a visual checkpoint before proceeding to centrifugation. The precipitate was centrifuged at 8000 rpm for 15 minutes and washed twice with distilled water and once with ethanol, with centrifugation at 8000 rpm for 10 minutes after each wash. The washed pellet was dried overnight at 60–70 °C and annealed at 250 °C for 3 hours to obtain ZnO nanoparticles powder.

Characterization

The synthesized ZnO nanoparticles were characterized using UV-Visible spectrophotometry over a wavelength range of 200–400 nm, with the sample dispersed separately in double-distilled water and methanol, to determine the wavelength of maximum absorption (λmax) and support nanoparticle synthesis [18]. FTIR analysis was performed on a KBr pellet of the dried nanoparticle powder over a wavenumber range of 4000–400 cm^{-1} to identify the functional groups associated with the phytochemicals on the nanoparticle surface and the Zn–O stretching vibrations consistent with ZnO formation. The UV–Visible and FTIR analyses were outsourced to an external analytical laboratory. The morphology of the dried powder was examined by scanning electron microscopy (SEM; secondary electron detector SE1, 20 kV accelerating voltage, 10.0 mm working distance, ×20,000 magnification; pixel size 14.65 nm). Particle length (longest dimension, maximum Feret diameter) was measured manually in ImageJ for n = 60 particles from a single micrograph, calibrated to the instrument pixel size, and expressed as mean ± SD. XRD, TEM and DLS/zeta potential analyses were not performed.

Antimicrobial Activity by Agar Well Diffusion Assay

Antimicrobial activity against *S. aureus* and *K. pneumoniae* was tested using the agar well diffusion method [19], modified from Alnehia et al. [12]. Sterile nutrient agar was prepared, autoclaved, and poured into Petri plates, and 100 µL of fresh bacterial culture was spread evenly over the surface using a sterile L-shaped spreader to form a uniform lawn. Wells about 6 mm in diameter were punched into the agar using a sterile cork-borer. Four concentrations of ZnO nanoparticle suspension — 20, 15, 10, and 5 mg/mL — were prepared, and 50 µL of each was added to its respective well, with a standard antibiotic disc used as the positive control. Plates were incubated at 37 °C for 24 hours, and antimicrobial activity was determined by measuring the zone of inhibition around each well in millimetres. Zone diameters were measured edge to edge and therefore include the 6 mm well diameter; ciprofloxacin (5 µg disc) was included as a reference only.

Evaluation of Antibiofilm Activity by Crystal Violet Assay

Antibiofilm activity against *S. aureus* and *K. pneumoniae* was evaluated using the crystal violet microtiter plate assay [20,21] modified from Shobha et al. [21]. Four stock concentrations of ZnO NP suspension (20, 15, 10, and 5 mg/mL, prepared by dilution of a 20 mg/mL stock) were used. In a sterile 96-well plate, 20 µL of bacterial culture and 20 µL of ZnO nanoparticle stock suspension at each stock concentration were

added along with LB broth to a final volume of 200 µL (tenfold dilution), giving final exposure concentration of 0.5, 1.0, 1.5 and 2.0 mg/mL, with an untreated well serving as control. Plates were incubated at 37 °C for 24 hours to allow biofilm formation, after which planktonic cells were removed and wells were washed with PBS and air-dried. Wells were stained with 0.1% crystal violet for 15–20 minutes, washed, and air-dried again, and the bound dye was dissolved in 95% ethanol for absorbance measurement at 570 nm. Reduction in crystal violet (CV)-stained biomass (%) was calculated relative to the untreated control, with all assays done in triplicate. Because the nanoparticles were added at inoculation, the assay measures reduced biofilm biomass formed in their presence, not eradication of preformed biofilms.

Limitations of the Study

XRD and TEM were not performed in this study, and SEM was limited to a single micrograph at ×20,000 in which particles and aggregates measured 164–1,083 nm and primary particles could not be resolved; hence direct evidence regarding the crystal phase, crystallite size and primary particle size of the synthesized nanoparticles could not be obtained. Additionally, the antimicrobial activity was assessed through a single agar well diffusion assay without replicates, while the antibiofilm assay was carried out in triplicate but without formal statistical significance testing between treatment groups. In addition, zone diameters include the 6 mm well and cannot be directly compared with the ciprofloxacin disc, and MIC was not determined. The crystal violet assay measured biomass formed in the presence of the nanoparticles without planktonic growth or viability controls, and only one strain per species was tested, so the findings should not be generalized to Gram-positive and Gram-negative bacteria as a whole. Future studies may incorporate XRD, TEM and higher-magnification SEM imaging, replicate antimicrobial testing, and statistical significance testing of the replicate data to further validate the present findings.

Conclusion

The present study demonstrates a simple and eco-friendly method for the green synthesis of zinc oxide nanoparticles using Punica granatum peel extract as a natural reducing and capping agent. FTIR analysis indicated the presence of phytochemical functional groups on the nanoparticle surface along with characteristic Zn–O vibrations, consistent with the formation of the nanoparticles. SEM showed particles and aggregates of 164–1,083 nm (mean 559 ± 217 nm); primary particle size and crystal phase (XRD) remain to be confirmed. The synthesized ZnO nanoparticles exhibited concentration-dependent zones of inhibition and reduced crystal-violet-stained biomass against *Staphylococcus aureus* and *Klebsiella pneumoniae*, with comparatively larger zones of inhibition observed against *K. pneumoniae*. Greater biomass reduction for *K. pneumoniae* was seen only at the two highest final concentrations (1.5 and 2.0 mg/mL), and results from one strain per species cannot be generalized to Gram-positive and Gram-negative bacteria. These preliminary findings suggest the potential of green-synthesized ZnO nanoparticles as an antimicrobial and biofilm-reducing agent, with future scope for structural characterization and further optimization of the synthesis process. MIC determination and viability controls are needed to confirm potency and antibiofilm action.

Data Availability

The datasets generated and/or analysed during the current study are available from the corresponding author on reasonable request.

Ethics Statement

This study did not involve human participants, human data, or vertebrate animals, and did not require ethics committee approval.

Conflicts of Interest

The authors declare no conflicts of interest.

Funding

This research did not receive any specific grant from funding agencies in the public, commercial, or not-for-profit sectors.

Abbreviations

AMR: Antimicrobial Resistance, EPS: Extracellular Polymeric Substance, FTIR: Fourier Transform Infrared Spectroscopy, KBr: Potassium Bromide, LB: Luria-Bertani broth, NaOH: Sodium Hydroxide, NP/NPs: Nanoparticle/Nanoparticles, OD: Optical Density, PBS: Phosphate-Buffered Saline, pH: Potential of Hydrogen, rpm: Revolutions Per Minute, SD: Standard Deviation, UV: Ultraviolet, UV-Vis: Ultraviolet-Visible Spectroscopy, SEM: Scanning Electron Microscopy, ZnO: Zinc Oxide, ZnO NPs: Zinc Oxide Nanoparticles, λmax: Wavelength of Maximum Absorption, *S. aureus*: *Staphylococcus aureus*, *K. pneumoniae*: *Klebsiella pneumoniae*, *P. granatum*: *Punica granatum*.

References

1. Luzala MM, Muanga CK, Kyana J, Safari JB, Zola EN, Mbusa GV, et al. A critical review of the antimicrobial and antibiofilm activities of green-synthesized plant-based metallic nanoparticles. Nanomaterials. 2022;12(11):1841. https://doi.org/10.3390/nano12111841
2. Kumarage PM, Gul T, Green NJ, Wardell SJT, Ali MA, Choudhury M, et al. Recent advances in gold and zinc oxide nanoparticles: antibiofilm action, mechanisms beyond ROS generation, and in vivo efficacy. Microbiol Res. 2026;306:128441. https://doi.org/10.1016/j.micres.2026.128441
3. Joudeh N, Linke D. Nanoparticle classification, physicochemical properties, characterization, and applications: a comprehensive review for biologists. J Nanobiotechnology. 2022;20:262. https://doi.org/10.1186/s12951-022-01477-8
4. Yahya H, Hamza A, Anas M, Alvi SK, Farheen A, Alam M. An extensive overview of nanoparticle classification, their applications and emerging horizons in nanotechnology. Biosci Biotechnol Res Asia. 2025;22(3):936-53. https://doi.org/10.13005/bbra/3416
5. Sirelkhatim A, Mahmud S, Seeni A, Kaus NHM, Ann LC, Bakhori SKM, et al. Review on zinc oxide nanoparticles: antibacterial activity and toxicity mechanism. Nano-Micro Lett. 2015;7(3):219-42. https://doi.org/10.1007/s40820-015-0040-x
6. Siddiqi KS, ur Rahman A, Tajuddin, Husen A. Properties of zinc oxide nanoparticles and their activity against microbes. Nanoscale Res Lett. 2018;13:141. https://doi.org/10.1186/s11671-018-2532-3
7. Miyanda P, Parveen Z. Role of plant phytochemicals in reduction, nucleation and stabilization of metallic nanoparticles in green synthesis. Int J Pharm Sci. 2026;4(4):2057-85. https://doi.org/10.5281/zenodo.19563304
8. Fouda A, Saied E, Eid AM, Kouadri F, Alemam AM, Hamza MF, et al. Green synthesis of zinc oxide nanoparticles using an aqueous extract of Punica granatum for antimicrobial and catalytic activity. J Funct Biomater. 2023;14(4):205. https://doi.org/10.3390/jfb14040205
9. Shaban AS, Owda ME, Basuoni MM, Mousa MA, Radwan AA, Saleh AK. Punica granatum peel extract mediated green synthesis of zinc oxide nanoparticles: structure and evaluation of their biological applications. Biomass Convers Biorefin. 2024;14(11):12265-81. https://doi.org/10.1007/s13399-022-03185-7
10. Hashem AH, Al-Askar AA, Saeb MR, Abd-Elsalam KA, El-Hawary AS, Hasanin MS. Sustainable biosynthesized bimetallic ZnO@SeO nanoparticles from pomegranate peel extracts: antibacterial, antifungal and anticancer activities. RSC Adv. 2023;13(33):22918-27. https://doi.org/10.1039/D3RA03260D
11. Hashem AH, El-Sayyad GS. Antimicrobial and anticancer activities of biosynthesized bimetallic silver-zinc oxide nanoparticles (Ag-ZnO NPs) using pomegranate peel extract. Biomass Convers Biorefin. 2024;14:20345- 57. https://doi.org/10.1007/s13399-023-04126-8
12. Alnehia A, Al-Odayni AB, Al-Sharabi A, Al-Hammadi AH, Saeed WS. Pomegranate peel extract-mediated green synthesis of ZnO-NPs: extract concentration-dependent structure, optical, and antibacterial activity. J Chem. 2022;2022:9647793. https://doi.org/10.1155/2022/9647793
13. Meshkatalsadat MH, Momeni A, Abdollahzadeh MR. Biosynthesis of zinc oxide nanoparticles using Punica granatum L. waste peel extract, and assessment of antioxidant and catalytic activity. Nano Biomed Eng. 2023;15(4):378-88. https://doi.org/10.26599/NBE.2023.9290030
14. Abdelmigid HM, Hussien NA, Alyamani AA, Morsi MM, AlSufyani NM, Kadi HA. Green synthesis of zinc oxide nanoparticles using pomegranate fruit peel and solid coffee grounds vs. chemical method of synthesis, with their biocompatibility and antibacterial properties investigation. Molecules. 2022;27(4):1236. https://doi.org/10.3390/molecules27041236
15. Zeghoud S, Hemmami H, Ben Seghir B, Ben Amor I, Kouadri I, Rebiai A, et al. A review on biogenic green synthesis of ZnO nanoparticles by plant biomass and their applications. Mater Today Commun. 2022;33:104747. https://doi.org/10.1016/j.mtcomm.2022.104747
16. Gadewar M, Prashanth GK, Ravindra Babu M, Dileep MS, Prashanth PA, Rao S, et al. Unlocking nature's potential: green synthesis of ZnO nanoparticles and their multifaceted applications – a concise overview. J Saudi ChemSoc. 2024;28:101774. https://doi.org/10.1016/j.jscs.2023.101774
17. Bitwell C, Indra SS, Luke C, Kakoma MK. A review of modern and conventional extraction techniques and their applications for extracting phytochemicals from plants. Sci Afr.

2023;19:e01585. https://doi.org/10.1016/j.sciaf.2023.e01585

18. Acosta-Humánez MF, Arrieta AA, Hernández J, Garay Y, Combatt EM, Libreros-Castillo KH, et al. An overview of basic characterization techniques for natural-originated biopolymers: UV-Vis and FTIR spectroscopy – a review. J Sci Technol Appl. 2025;18:106. https://doi.org/10.34294/j.jsta.25.18.106
19. Lage OM, Ramos MC, Calisto R, Almeida E, Vasconcelos V, Vicente F. Current screening methodologies in drug discovery for selected human diseases. Mar Drugs. 2018;16(8):279. https://doi.org/10.3390/md16080279
20. Amran SSD, Syaida AAR, Mat Jalil MT, Mohamad Nor NH, Raja Yahya MFZ. Preparation of biofilm assay using 96-well and 6-well microplates for quantitative measurement and structural characterization: a review. Sci Lett. 2024;18(2):121-34. https://journal.uitm.edu.my/index.p hp/ScL/article/view/6555
21. Shobha B, Ashwini BS, Ghazwani M, Hani U, Atwah B, Alhumaidi MS, et al. Trichoderma-mediated ZnO nanoparticles and their antibiofilm and antibacterial activities. J Fungi. 2023;9(2):133. https://doi.org/10.3390/jof9020133
22. Mohammadi A, Hashemi N, Ghassabzadeh M, Sharafi A, Yazdinezhad A, Danafar H. Green synthesis and toxicological evaluation of zinc oxide nanoparticles utilizing Punica granatum fruit peel extract: an eco-friendly approach. Sci Rep. 2025;15:20853. https://doi.org/10.1038/s41598-025-05544-6
23. Rutherford D, Šlapal Bařinková M, Jamatia T, Šuly P, Cvek M, Rezek B. Capping agent control over the physicochemical and antibacterial properties of ZnO nanoparticles. Appl Surf Sci. 2025;692:162739. https://doi.org/10.1016/j.apsusc.2025.162739
24. Li Y, Liao C, Tjong SC. Recent advances in zinc oxide nanostructures with antimicrobial activities. Int J Mol Sci. 2020;21(22):8836. https://doi.org/10.3390/ijms21228836